Heliyon 10 (2024) e37934

Contents lists available at ScienceDirect

Heliyon

journal homepage: www.cell.com/heliyon

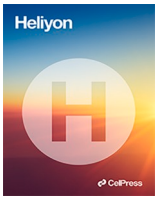

Research article

# Two marine sulfur-reducing bacteria co-culture is essential for productive infection by a T4-like *Escherichia coli*-infecting phage

Adriele Jéssica do Carmo Santos [a,1], Roberto Sousa Dias [b,1], Jéssica Duarte Silva [a], Maíra de Paula Sousa [c], Wellington Ronildo Clarindo [b], Cynthia Canêdo da Silva [a], Sérgio Oliveira de Paula [b,*]

[a] *Department of Microbiology, Federal University of Viçosa, Avenue Peter Henry Rolfs, s/n, Viçosa, Minas Gerais, 36570-900, Brazil*
[b] *Department of General Biology, Federal University of Viçosa, Avenue Peter Henry Rolfs, s/n, Viçosa, Minas Gerais, 36570-900, Brazil*
[c] *Leopoldo Américo Miguez de Mello Research and Development Center, Petrobras, Av. Horácio Macedo, 950, Federal University of Rio de Janeiro, Rio de Janeiro, 21941-915, Brazil*

A R T I C L E I N F O

*Keywords:*
Microbiologically influenced corrosion
Biofilm
Bacteriophage
Phage biology

A B S T R A C T

The control of microbiologically influenced corrosion (MIC) challenges the oil exploration sector. The MIC results from electrochemical reactions facilitated by microorganisms such as sulfate-reducing bacteria (SRB), which adhere to the surface of the ducts forming biofilms. SRB uses sulfate as the final electron acceptor, resulting in hydrogen sulfide as the final product, a highly reactive corrosive, and toxic compound. Due to the high diversity of the SRB group, this study evaluated the effect of an *Escherichia coli* phage, with biofilm degrading enzymes, in preventing biofilm formation by microbial consortium P48SEP and reducing $H_2S$ production in a complex SRB community. Three phage concentrations were evaluated ($10^4$, $10^8$ and $10^{12}$ UFP/ml). High and medium phage concentrations prevented biofilm development, as evidenced by scanning electron microscopy, chemical analysis, and cell counts. In addition, the virus altered the expression pattern of some bacterial genes and the relative abundance of proteins related to biofilm formation and cell stress response. Using a complex culture formed mainly by SRB, it was possible to observe the bacterial growth, $H_2S$, and metabolic activity reduction after the phage was added. This study shows for the first time the ability of an *E. coli*-infecting phage to prevent the biofilm formation of an SRB consortium and infect and replicate at high concentrations on the non-specific host. This new finding turns the use of non-specific phages a promising alternative for the control of biocorrosion in oil and gas installations, on the other side, alert to the use of large concentration of phages and the influence on bacterial groups with geological importance, opening a research field in phage biology.

## 1. Introduction

Oil demand has increased dramatically in recent decades, being the world's leading energy source [1]. However, oil pipelines and associated infrastructures are subject to different corrosion mechanisms, one of which is microbiologically influenced corrosion (MIC)

* Corresponding author.
*E-mail address:* depaula@ufv.br (S.O. de Paula).
[1] These authors contributed equally.

https://doi.org/10.1016/j.heliyon.2024.e37934
Received 21 February 2024; Received in revised form 5 September 2024; Accepted 13 September 2024
Available online 14 September 2024

or biocorrosion, which causes significant economic losses for sector [2]. The MIC results from a series of electrochemical reactions, influenced or directly caused by microorganisms, which adhere to the surface of the pipes and eventually form the biofilms [3]. The biocorrosion process is estimated to account for 20–40 % of severe corrosion cases in oil exploration and transport. In addition, about 70–95 % of internal pipeline leaks are mainly caused by MIC [4,5].

The biofilms are formed mainly by a matrix of exopolysaccharides, proteins, and nucleic acids and turn bacteria more resistant to biocides and physical removal, protecting microbial cells from the external environment [6–8]. The deeper layers of mature biofilms (nearest to the adhered surface) are predominantly anaerobic due to oxygen consumption by aerobic microorganisms in the surface layers, creating an ideal environment for sulfate-reducing bacteria (SRB). The SRB constitutes the principal group of microorganisms responsible for MIC [9,10] and can reduce sulfate to hydrogen sulfide ($H_2S$), a highly toxic and corrosive product of the SRB metabolism. Iron sulfide (FeS) is formed by the chemical reaction between $H_2S$ and the iron present in steel. The FeS formed inside the pipes ends up being precipitated, which causes the clogging of metallic structures, such as oil pipelines and reservoirs, generating significant losses [11]. Furthermore, a high concentration of $H_2S$ in the oil storage tanks and pipelines promotes oil acidification, known as souring.

The oil industries are constantly looking for new strategies that can control or prevent the formation of biofilms, reducing the economic losses caused by MIC and mitigating the environmental impacts. There are limited effective strategies to inhibit biofilm and MIC growth in petroleum-related environments, with chemical biocides being the most used method [12]. However, biocides have difficulty penetrating the biofilm matrix and reaching the microorganisms in the deep biofilm layer. In addition, biocides are expensive, can lead to the generation of resistant bacteria, and represent a significant risk to humans and the environment due to their toxicity and persistence in industrial waste [13,14]. An attractive alternative to chemical biocides is solutions based on bacteriolytic agents called bacteriophages [15,16].

Most phages have genes in their genome that encode depolymerase, hydrolases, and lytic proteins (lysins) that act as adjuvants for phage infection and enable biofilm matrix degradation, allowing bacteriophages access to the initially inaccessible cell receptors on the bacterial surface. In addition, planktonic bacteria are more susceptible to the action of antibiotics and other antimicrobial agents, such as chemical biocides used to control and prevent biofilms [16–19]. There are few studies about the use of bacteriophages in the control of sulfate-reducing bacteria (SRB) [20], and due to the large number of species that make up the SRB group [21,22], the isolation of specific phages for each species becomes unfeasible. Therefore, isolated phages for aerobic bacteria that affect the growth of SRB and other anaerobic organisms are extremely advantageous as they facilitate the propagation process and reduce production time and cost.

Phage vB_EcoM-UFV13 (UFV13) is a member of the *Tequatrovirus* genus, presenting a wide range of hydrolases in its genome. It is believed that a large amount of virion-associated peptidoglycan hydrolases (VAPGS) may interfere with biofilm formation by interacting and degrading the polymeric substances present in the biofilm matrix [23,24]. Indeed, T4-like phages are extremely widespread, and occasionally dramatic changes in the host range can occur [25]. Due to these characteristics, we evaluated the influence of phage vB_EcoM-UFV13 on biofilm formation by the SRB consortium P48SEP in a carbon steel coupon. Our results showed that phage was able to reduce biofilm in a dose-dependent manner. Several analyses were performed to establish the mechanisms, and together, revealed the ability of phage to decrease bacterial growth and replicate at high concentrations in the consortium only.

## 2. Materials and methods

### 2.1. SRB consortium and biofilm assay

The consortium P48SEP was isolated from the production water of an oil extraction platform in the Campos Basin, Rio de Janeiro, Brazil. The consortium was inoculated in Postgate C medium [26] (without $FeSO_4$) and incubated in the anaerobic environment at 30 °C. The optical density (O.D.600) was monitored using a DR3900 spectrophotometer (Hach, Loveland, CO, USA) for 15 days.

To analyze the bacterial composition of the consortium, the DNA was extracted as described by Pospiech & Neumann [27]. After the extraction, the genetic material was subjected to a polymerase chain reaction (PCR) using the 10f and 1100r primers (Supplementary Table 1) [28]. The amplicons were purified using the Promega Wizard® SV Gel and PCR Clean-Up System kit (Promega, Madison, WI, USA) following the manufacturer's recommendations and sequenced. The sequence obtained was compared with those deposited in the GenBank database (http://www.ncbi.nlm.nih.gov) using the BLASTn platform (https://blast.ncbi.nlm.nih.gov/Blast.cgi). The sequences were aligned using the CLUSTALW [29] and analyzed with the MEGA 7.0.18 software [30]. Subsequently, the Neighbor-Joining method built a phylogenetic tree with a 1,000× bootstrap.

### 2.2. Bacteriophage vB_EcoM-UFV13

The vB_EcoM-UFV13 belongs to the bacterial virus collection of the Laboratory of Molecular Immunovirology, Federal University of Viçosa (Minas Gerais, Brazil), and it has the enzymatic capability previously described [23,24]. Viral titer was determined using a well-established double-layer protocol [31], using the original host *Escherichia coli* 30.

To evaluate the influence of vB_EcoM-UFV13 phage on biofilm formation by the consortium P48SEP, three different phage concentrations were evaluated, (i) treatment with low phage concentration $10^4$ PFU/mL, (ii) medium concentration $10^8$ PFU/mL, and (iii) high concentration $10^{12}$ PFU/mL.

### 2.3. Biofilm analyses

#### 2.3.1. Steel coupons

In this work, carbon steel coupons were used, with different surface areas (hereafter called coupon A - 1 $cm^2$ and coupon B - 6 $cm^2$). At one end of the coupons, a hole was made through which the coupons were suspended by a nylon thread (Supplementary Fig. 1). Before each test, the coupons were blasted with 200 μm glass microspheres, using a blaster with a pressure of 60 lbs (Protecni, Araraquara, SP, Brazil), to remove impurities or scale [32]. The coupons were sterilized by ultraviolet radiation (40 cm distance, 15W UV light) for 30 min on each side.

#### 2.3.2. Biofilm formation

Biofilm formation by the consortium P48SEP was evaluated in the presence and absence of bacteriophage. The experimental systems were assembled in 30- and 90-mL flasks (Supplementary Fig. 1), containing modified Postgate C medium and the inoculated bacteria ($OD_{600}$ 0.1). The flasks were anaerobically conditioned at 30 °C for 15 days. The phage was inoculated at different concentrations according to treatments 1, 2, and 3 ($10^4$, $10^8$, and $10^{12}$ PFU/mL).

#### 2.3.3. Scanning electron microscopy (SEM)

The coupons A containing the biofilm were washed 3 times in PBS 1× pH 7.4 and fixed in paraformaldehyde 3.7 % (v/v) at room temperature for 12 h. Coupons were dehydrated in increasing ethanol series (30–100 % v/v) for 10 min each step and repeated three times in ethanol 100 %. Then coupons were subjected to a critical point dryer (CPD, Bal-tec®, model 030, Germany) and covered with gold (Sputter coater, Balzers, model FDU010, Germany). Finally, the coupons were examined on the Leo 1430 VP Scanning Electron Microscope at the Núcleo de Microscopia e Microanálise (Center for Microscopy and Microanalysis), operating at 20 kV [33].

#### 2.3.4. Extracellular polymeric substance (EPS) extraction

The biofilm formed in coupons B were scraped and suspended in PBS 1× buffer, forming a biofilm-derived suspension (BDS). EDTA extraction was used for EPS extraction by adding 1 mL of EDTA solution 2 % (w/v) to every 1 mL of BDS. The mixture was stirred for 12 h at 4 °C. Thereafter, samples were filtered on 0.22 μm membrane and dialyzed against deionized water using a 3.5 kDa dialysis membrane Spectra/Por® (Fisher Scientific, Göteborg, Sweden) the water was changed twice, every 1 h and a third exchange was made at 12 h [34].

#### 2.3.5. Biomolecules quantification

Carbohydrates, proteins, and extracellular DNA (eDNA) were quantified in the BDS. Carbohydrate concentrations were determined using the phenol/sulfuric acid method, using D-glucose as standard [35]. For the determination of protein concentration, the bicinchoninic acid assay (BCA) was performed using commercial kits (Thermo Fisher Scientific, Waltham, MA, USA) and bovine serum albumin (BSA) as standard [34]. Extracellular DNA was quantified using the Qubit® dsDNA BR reagent kit (Invitrogen, Carlsbad, CA, USA) and DNA-λ as standard [33,34].

#### 2.3.6. Cell count

The number of living cells (live/dead assay) present in the biofilm was determined by the live/dead approach using propidium iodide (10 μg/mL) and FITC (2 μg/mL) staining for 5 min. After this incubation, the biofilm was fixed with paraformaldehyde 3.5 % (v/v) for 5 min. The coupons were then washed with PBS buffer and placed in the ultrasound bath for 8 min to detach the biofilm, allowing the number of cells present in it to be evaluated, and then the solution was centrifuged at low speed (600×*g*, 5 min) to precipitate the products of corrosion. The supernatant was transferred to new tubes and immediately analyzed in the flow cytometer BD Accuri™ C6 (BD Biosciences, USA), equipped with two lasers (one blue at 488 nm and one red at 640 nm). Bacteria stained with propidium iodide were detected using the FL3 detector (610 ± 20 nm), and bacteria stained with FITC by the FL1 detector (530 ± 30 nm). Data were analyzed using BD Accuri™ C6 software (BD Biosciences).

#### 2.3.7. Evaluation of enzymatic effects

The biofilm was pre-formed for 15 days at 30 °C on steel coupons and submitted to the enzymatic treatment with DNase and proteinase K to evaluate the role of eDNA and proteins in their stability. Initially, the biofilms were washed with PBS 1× before adding 100 μg/mL DNase in the specific buffer (400 mM Tris-HCl pH 8.0, 100 mM $MgSO_4$, 10 mM $CaCl_2$) and incubated at 37 °C for 1 h. After treatment, the biofilms were rewashed three times to remove traces of the enzyme. Then, the adhered cells were stained with propidium iodide (10 μg/mL) and FITC (2 μg/mL) and quantified by flow cytometry as described in topic 2.3.6. The same procedure was performed on new coupons using 10 μg/mL of proteinase K in a specific buffer (20 mM Tris-HCl pH 8.0, 100 mM NaCl).

#### 2.3.8. Proteomic analysis

The biofilm was extracted according to item 2.3.4, lyophilized, and sent to GenOne (Rio de Janeiro, RJ, Brazil), where it was subjected to protein extraction, quantification, and digestion by trypsin after cleavage of the proteins, the samples were submitted to LCMS-NanoUltra-HPLC ultimate 3000 and Quadropole-Orbitrap QExactive Plus Gradient for 65 min. Finally, the Proteome Discoverer program (Thermo Fisher Scientific, Waltham, MA, USA) was used to identify proteins. The Exponentially Modified Protein Abundance Index (emPAI) was used to compare the proteins in the treatments and control. The emPAI value is proportional to protein abundance in a protein mixture [36].

### 2.4. Phage-consortium interactions

#### 2.4.1. Adsorption assay

An adsorption assay was performed to evaluate if, besides enzyme action on biofilm, the phage could act directly on the bacterial surfaces. Briefly, the phage ($10^{12}$ PFU/mL) was previously stained with SYBR® Gold (Thermo Fisher Scientific, Waltham, Massachusetts, USA) in a ratio of 100:0.01 (vol/vol) and incubated overnight in the darkroom at 4 °C. SYBR-labeled phages were then mixed 1:1 (vol/vol) with cells of the P48SEP consortium for 1.5 h at 30 °C. After incubation, the bacterial culture was visualized on the EVOS M5000 microscope (Thermo Fisher Scientific). The presence of fluorescent cells confirmed the phage adsorption [37,38]. Some controls were performed in this experiment. First, the P48SEP consortium was incubated with a solution of SYBR® Gold at a ratio of 100:0.01 (vol/vol) and incubated for 1.5 h at 30 °C. The second control was the bacterial consortium without staining to evaluate the presence of proper fluorescence. Furthermore, the analysis was carried out for each species present in the consortium separately.

#### 2.4.2. Gene expression

*2.4.2.1. Bacterial genes.* Gene expression was evaluated to verify the influence of phage action on bacterial metabolism under the three different treatments. Thus, genes responsible for biofilm formation (Pbp, Gt, and Gs), genes involved in the capture, transport and storage of iron in cells (*bfr*, and *feo*B), present in the genome of *O. marinus* were selected for analysis. The *gyrase* A (*gyr*A) gene was used as endogenous control. The other primers used for gene expression analysis were designed using Primer Express Software 3.0 (Thermo Fisher Scientific, Waltham, MA, USA) based on the genomic sequence of *O. marinus* deposited in GenBank under accession number NZ_QMIF01000001.1. All primer sets were evaluated using Oligo Analyzer 1.0.2 software, and specificity was estimated by the Primer-BLAST tool. The primer sets are described in Supplementary Table S1.

RNA was obtained using a commercial extraction solution with a previous mechanical cell lysis step. In a microtube containing 0.5 g zirconium beads (0.1 mm diameter) were added 1 mL of BDS, 20 % SDS solution (w/v), and 0.7 mL of Trizol® (Invitrogen, Carlsbad, CA, USA). The mechanical lysis was performed on the Bead Ruptor (Omni International, Kennesaw, GA, USA) homogenizer for 1 min. The tubes were incubated at 60 °C for 30 min, subjected to second mechanical lysis under the same condition, and centrifuged (12,000×*g*, 10 min, 4 °C). The aqueous phase was transferred to new tubes and subjected to RNA extraction using the Trizol® Reagent (Sigma-Aldrich, St. Louis, MO, USA). The RNA obtained was treated with DNase using an RQ1 RNase-Free DNase kit (Promega, Madison, WI, USA), following the manufacturer's instructions. RNA's concentration and purity were estimated in Nanodrop ND-2000 (Thermo Fisher Scientific, Waltham, MA, USA). The RNA integrity was analyzed by 1 % agarose gel electrophoresis stained with ethidium bromide in TBE 1× buffer and observed under ultraviolet light. GoScript Reverse transcription System (Promega, Madison, WI, USA) synthesized complementary DNA (cDNA). The amplification of gyrase previous to the reverse transcription step was used as a control of DNase treatment.

Initially, qPCR efficiency was evaluated using SsoFast® EvaGreen Supermix (Bio-Rad Laboratories, Hercules, CA, USA). The final reaction volume was 20 μL, containing 1× SsoFast® EvaGreen supermix, primer at 200 nM final concentration, and cDNA sample at different concentrations (5; 0.5; 0.05; 0.005 ng). Assays were performed in triplicate on the Eco® Real-Time PCR system (Illumina, San Diego, CA, USA). The final qPCR reaction conditions were 40 cycles, being the denaturation at 95 °C for 30 s, annealing at 56 °C for 60 s, and elongation at 72 °C for 60 s, using primers for the bacterial gyrase A genes (*gyr*A).

*2.4.2.2. Phage genes.* To assess if the genes of the vB_EcoM-UFV13 phage were transcribed into the cells present in the consortium, the total RNA was extracted from the culture 90 min after phage contact. The RNA was treated with DNase and used to obtain the cDNA. The cDNA was used in the common PCR reaction with primers for five different genes, two structural (cap and tail fiber), two non-structural (helicase and phage sigma factor), and bacterial gyrase (*gyr*A) as control (Supplementary Table 1).

### 2.5. Bacterial growth curve

After evaluating the influence of bacteriophages on the biofilm and the ability to adsorb and interfere with the expression of bacterial genes, we sought to assess the effect on the growth of bacterial isolates and the consortium. The consortium was previously cultured for 24 h. This process was repeated three times to achieve a fully activated culture. Afterward, the isolates and bacterial consortium were cultured in the presence of phage at the three different concentrations. All cultures were started at $OD_{600}$ 0.1, and the growth was accompanied for 15 days using a DR3900 spectrophotometer.

### 2.6. Evaluation of productive infection

The capacity of phage vB_EcoM-UFV13 to infect and replicate in bacteria present in the consortium P48SEP was evaluated. The tubes were incubated for 15 days in anaerobic conditions at 30 °C, and the growth curve was monitored, as previously mentioned (Topic 2.5). Tubes containing Postgate C medium were inoculated with culture at final $OD_{600}$ 0.1, and the virus was inoculated at the concentration of $10^{12}$ PFU/mL. Samples were collected at 30 min intervals, filtered in 0.22 nm pore membrane, and titrated in the original host *Escherichia coli* 30.

### 2.7. Pilot-scale assay

The results obtained with consortium P48SEP were evaluated in a complex community on a pilot scale. An established culture (UORio), gently provided by Cenpes/Petrobras, comes from a mixture of water from different platforms and the injection water catchment maintained in anaerobioc conditions in Postgate E medium without $Fe^{+}$ supplementation. This complex culture was expanded to 400 mL (5 % total volume of the tank) and added to a hermetically closed tank containing 6.8 L of synthetic seawater (0.003 g NaF, 0.02 g $SrCl_2.6H_2O$, 0.03 g $H_3BO_3$, 0.1 g KBr, 0.7 g KCl, 1.113 g $CaCl_2.2H_2O$, 4 g $Na_2SO_4$, 10.78 g $MgCl_2.6H_2O$, 23.5 g NaCl, 0.02 g $Na_2SiO_3.9H_2O$, 0.001 g $Na_4EDTA$ and 0.2 g $NaHCO_3$ per liter) supplemented with 800 mL of nutritive solution (4 mL sodium lactate (50 %)), 1 g yeast extract, 0.25 g glucose, and distilled water to complete 1 L). The unpurified bacteriophages UFV13 and a previously described T7-like bacteriophage [39] were added at ~$10^8$ PFU/mL, and the control solution (residual culture medium after bacterial growth at the same conditions to phage production) was added to the tank at the beginning of the exponential growth of the culture, at an equal volume of the treatments. The bacterial growth was assessed by optical density and metabolic state by $H_2S$ production [40], and ATP quantification using a luminometer (LuminUltra Photonmaster, HACH Loveland, CO, USA) [41]. The ATP was quantified three times during the experiment, the first at the beginning, the second one day after the phage inoculum, and the end of the experiment (18° day). All other parameters were monitored for 18 days.

### 2.8. Statistical analysis

All treatments in this work were performed in triplicate. Statistical analysis was performed using GraphPad® software version 9.3.1 (GraphPad, La Jolla, CA, USA), using one-way analysis of variance (ANOVA) with 95 % accuracy to evaluate the significance in the differences between the control and treatments, and Tukey's test to multiple comparisons.

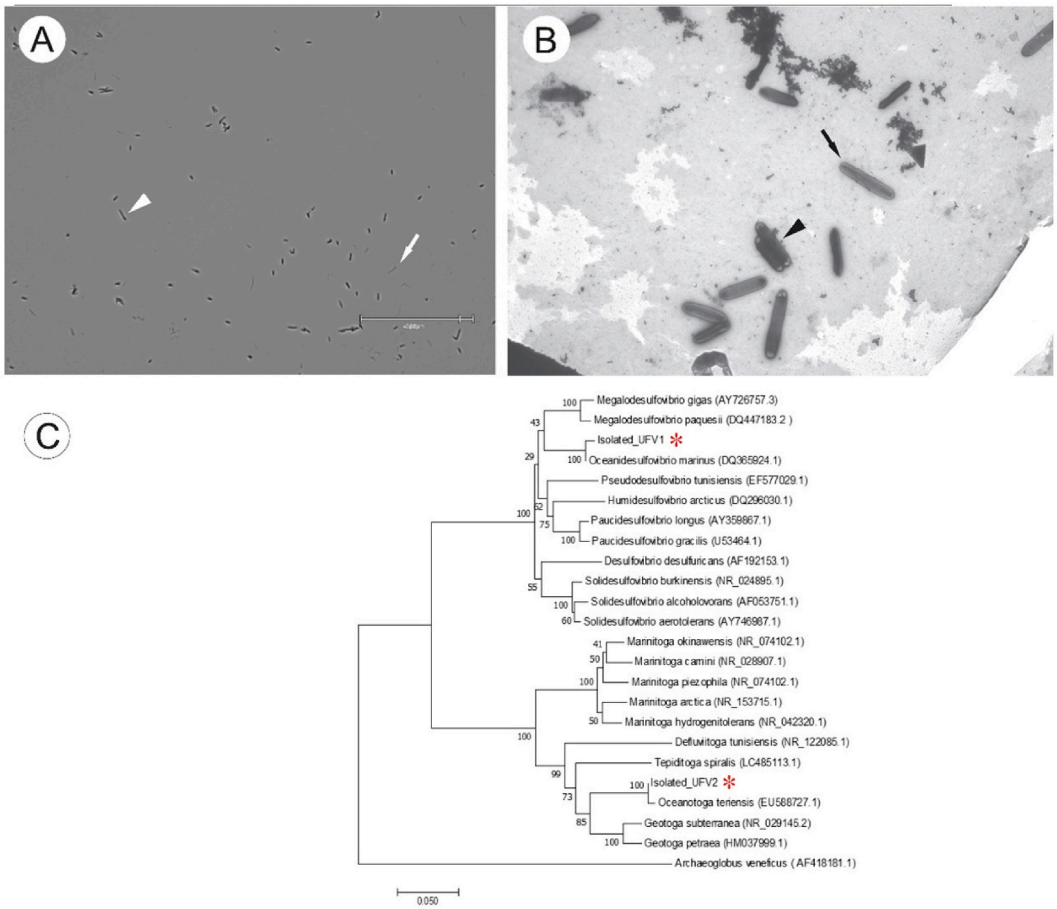


**Fig. 1. Phylogenetic analysis.** A) Light microscopy and B) Transmission electron microscopy (TEM), both from the P48SEP consortium; the arrowhead points to *Oceanotoga teriensis,* an arrow indicating the *Oceanidesulfovibrio marinus.* C) Phylogenetic tree based on the partial sequence of the 16S rRNA of the isolates UFV1 (*O. marinus*) and UFV2 (*O. teriensis*), both marked with a red asterisk. The tree was built using the Neighbor-Joining method with Bootstrap value represented in the branches for 1000 repetitions. The sequence accession number in the GenBank is shown in parentheses.

## 3. Results

### 3.1. Identification and phylogenetic analysis using the 16S rRNA

The P48SEP consortium was identified as formed by two bacteria presenting different morphologies (Fig. 1A and B). Using optical microscopy, it is possible to verify the presence of two distinct bacteria (Fig. 1A). The bacterium *O. teriensis* showed greater contrast, with a dark color, indicated in the figure by the arrowhead. While *O. marinus* has a grayish color and lower contrast, indicated by the arrow, but both show the formation of bacilli. The differences are more evident in transmission electron microscopy (Fig. 1B), *O. teriensis* cells have a structure known as a toga at their ends, this structure is a characteristic of the *Petrotogaceae* family. Such a structure is not observed in *O. marinus* cells. Being the most abundant SRB *Oceanidesulfovibrio marinus* (named *O. marinus* P48SEP P48SEP_1 GenBank number NZ_QMIF01000001.1), and the second isolate was identified as *Oceanotoga teriensis* UFV_LIMV02 (16S rRNA partial sequence, accession number MW349105.1). The phylogenetic analysis using the 16S rRNA gene confirms the taxonomic identification of the isolates (Fig. 1C). The alignment of the sequences of the isolates with the sequences of the GenBank database revealed that the P48SEP_1 isolate is related to members of the genus *Oceanidesulfovibrio* with 100 % identity with the species *Oceanidesulfovibrio marinus* (accession number DQ365924.1). The second UFV2 isolate aligned with 100 % identity with the *Oceanotoga teriensis* species (accession number EU588727.1).

### 3.2. Biofilm morphology analysis in carbon steel coupons

The SEM imaging was performed to evaluate the influence of phage vB_EcoM-UFV13 on the morphology of biofilm formed on the surface of coupons (Fig. 4A–D). The biofilm formed in the absence of the virus (Fig. 2A) has extensive extracellular material (EPS), forming a dense biofilm with bacterial clumps. The EPS allows the creation of a non-homogeneous and porous biofilm on the metal surface, promoting water flux and physical-chemical changes, creating a favorable environment for the electrochemical reactions responsible for localized corrosion known as pits [42]. Although the phage UFV13 has decreased bacterial growth only at higher concentrations, treatments with medium and high phage concentrations (Fig. 2C and D) effectively decreased the biofilm formed. There was a reduction in biofilm in the lower titer ($10^4$ PFU/mL) (Fig. 2B), but less significant in the other 2 treatments.

### 3.3. Biofilm composition analysis

Given the importance of the three main components of the bacterial biofilm matrix, polysaccharide, protein, and extracellular DNA content in the biofilm were quantified. In the presence of phage at the two higher concentrations ($10^8$ and $10^{12}$ PFU/mL) was possible to observe a significant decrease in carbohydrate and protein concentration in BDS, but not when was used the lower concentration ($10^4$ PFU/mL) (Fig. 3A and C). Contrariwise, there was a slight increase in the carbohydrate concentration in the matrix at this concentration. At the same time, the quantification of extracellular DNA showed a significant reduction in the three treatments (Fig. 3B).

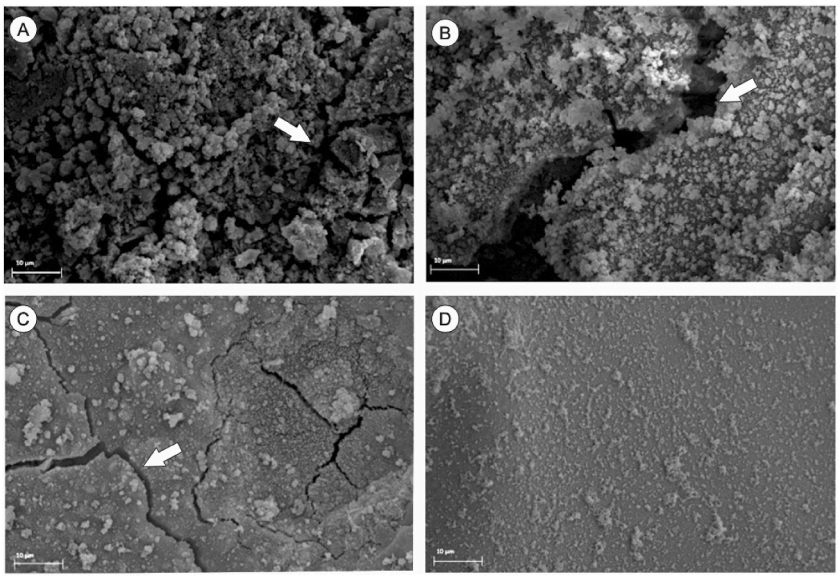


**Fig. 2. Scanning electron microscopy (SEM)**. Micrographics of biofilms formed by the bacterial consortium on the carbon steel surface in the presence of vB_EcoM-UFV13 and their absence (control) at 3500× magnification. White arrows show cracks on the surface of biofilm (A and B) and the metal (C). A) absence of phage (control) and presence of phage at B) concentration $10^4$; C) $10^8$; D) $10^{12}$ PFU/mL. Bars represent 10 μm.

### 3.4. Cell count

Flow cytometry assessed the number of viable cells in biofilms formed at different concentrations of vB_EcoM-UFV13. A significant decrease was observed in the number of live cells adhered to the coupon surface in the presence of phages at concentrations of $10^8$ and $10^{12}$ PFU/mL (Fig. 3D); compared to the control. No significant changes were observed in the treatment with low viral concentration.

### 3.5. Proteomic analysis

Proteomic analysis was performed from samples of biofilm treated with different concentrations of vB_EcoM-UFV13 and untreated (control) to evaluate possible changes in the protein composition in the extracellular polymeric substance that constitutes the biofilm. One hundred eighty-three proteins were detected from both species in the consortium P48SEP (Supplementary Table 2). However, twelve proteins related to biofilm formation and stress response were selected from differentially expressed proteins for quantitative analysis, four proteins related to *O. teriensis* (S-layer, ABC transport, peptide/nickel transport and flagellin) and eight proteins belonging to *O. marinus* (60 kDa chaperonin, extracellular solute-binding, Omp, extracellular ligand-binding, sulfate adenylyl-transferase, molybdenum ABC transporter, periplasmic [NiFe] hydrogenase and sulfite reductase) (Fig. 4).

Almost all proteins found had their relative amounts affected by the presence of the bacteriophage (Fig. 4); however, although some proteins had visible changes, these changes were not statistically significant.

### 3.6. Adsorption capacity

Given the dramatic changes caused on biofilm by phage, we evaluated the possibility of the phage being adsorbed by some bacteria in the consortium. Although this phage is not specific to any bacteria in the consortium, fluorescence microscopy revealed that the phage was being adsorbed by one of the two cells that make up the P48SEP consortium (Fig. 5A). SYBR Gold I is a dye capable of penetrating the capsids of bacteriophages and intercalating into their nucleic acid [43]. The consortium's fluorescence was evaluated when placed in contact only with SYBR Gold and the consortium's own autoflowering P48SEP (Fig. 5B and C), in both situations, did not show fluorescence. When separately analyzing the species that make up the consortium, in the presence of vB_EcoM-UFV13 previously stained with SYBR Gold, it revealed that the fluorescence is visible only for the species *O. marinus* (Fig. 5D), while the second species *O. tereinsis* did not show fluorescence (Fig. 5E). Showing that phage vB_EcoM-UFV13 is capable of binding to and

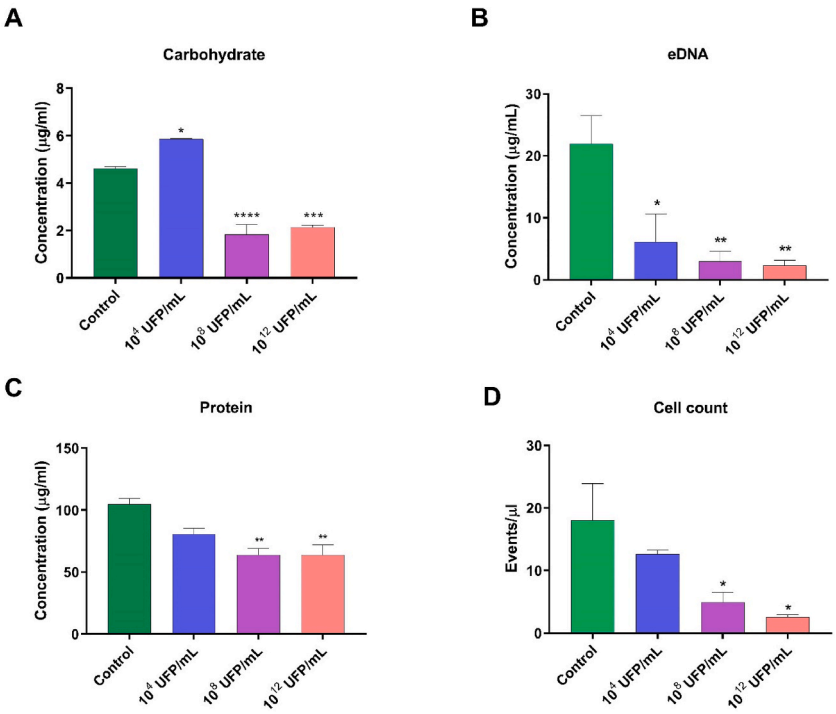


**Fig. 3. Biofilm composition.** A) Quantification of sugar, B) DNA, and C) protein in carbon steel coupon biofilms in the absence of phage (control) or in the presence of vB_EcoM-UFV13 at concentrations of $10^4$, $10^8$, and $10^{12}$ PFU/mL. Bars represent the standard deviation. Statistically significant differences when compared to control (*P < 0.05, **P < 0.01, ***P < 0.001), (n = 3). D) Quantification of viable cells in the P48SEP bacterial pool formed in carbon steel coupons without phage (control) or in the presence of vB_EcoM-UFV13 at $10^4$, $10^8$, or $10^{12}$ PFU/mL concentrations. Error bars represent standard deviation. Statistically, differences when compared to the control (*P < 0.05), (n = 3).

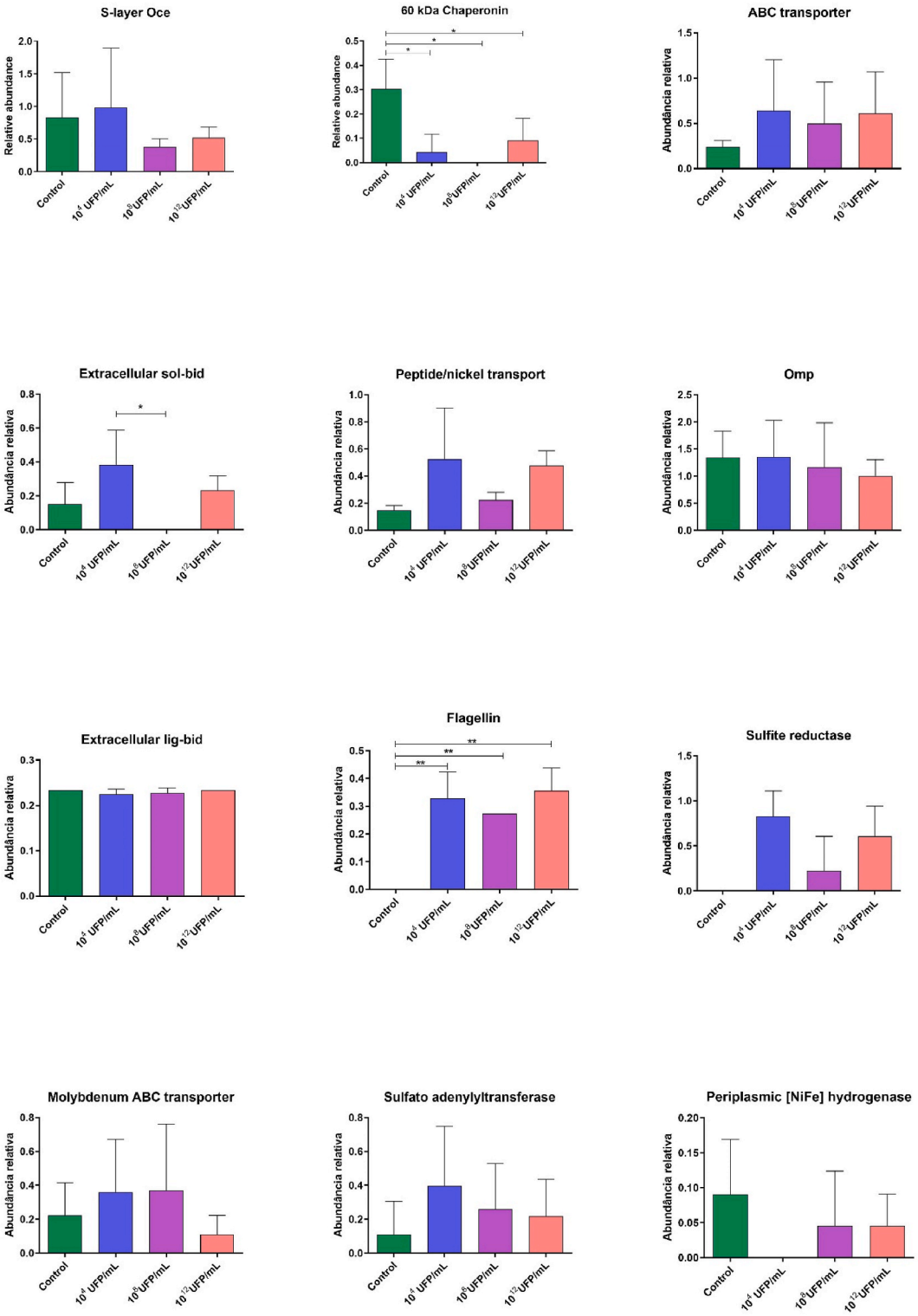


**Fig. 4. Biofilm proteomics.** Relative abundance of *Oceanotoga teriensis* and *Oceanidesulfovibrio marinus* proteins in the biofilm. The values observed on the Y axis refer to the Exponentially Modified Protein Abundance Index (emPAI), which provides approximate relative quantification. Statistical differences when compared to the control (*$P < 0.05$, **$P < 0.01$), ($n = 3$).

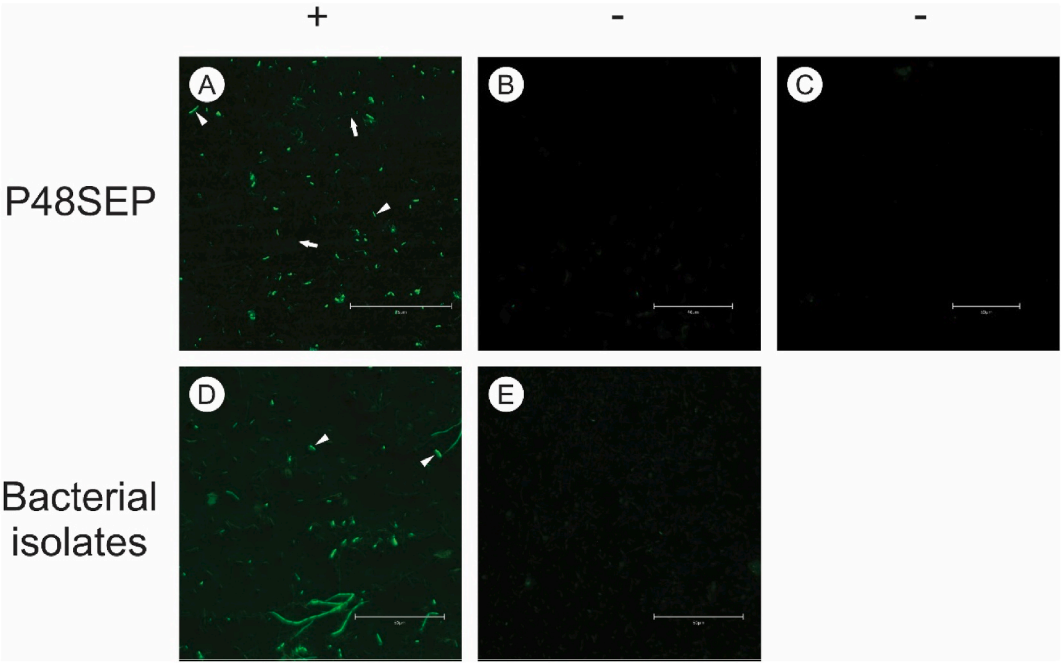


**Fig. 5. Adsorption assay.** A) P48SEP treated with phage previously labeled with SYBR. Fluorescence microscopy of *O. marinus* bright (arrowhead) due to adsorption of phage labeled with SYBR, and *O. teriensis* (arrow) opaque, indicating non-adsorption of the phage; B) P48SEP incubated with SYBR alone; C) Only the P48SEP consortium, to evaluate autofluorescence; D) *O. marinus* alone incubated with labeled phage; and E) *O. teriensis* alone incubated with labeled phage. The + sign indicates the presence of fluorescence, while the – sign indicates the absence of fluorescence.

adsorbing by *O. marinus*.

### 3.7. Gene expression

One principal component of the biofilms reported in the literature is carbohydrates [44]. They assist in the cell adhesion process and protect cells against antimicrobial agents. Knowing their importance, three genes involved in the polysaccharide synthesis and transport pathway were selected.

The expression of carbohydrate biosynthesis-related genes (Pbp, Gs, and Gt) by cells in biofilms submitted to medium and high phage concentrations did not present significant alterations in control (Fig. 6). There was a significant increase in expression levels of all genes evaluated in the cells present in the biofilm treated with low phage content (treatment $10^4$ PFU/mL), when compared to the control.

The phage genes were also expressed. However, although structural genes were amplified, the sigma factor could not be detected (Supplementary Fig. 2).

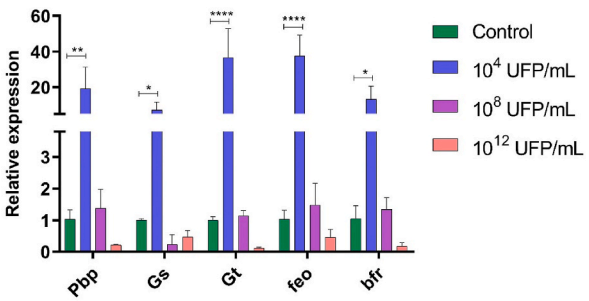


**Fig. 6. Transcription analyses.** Evaluation of transcriptional expression of genes: exopolysaccharide biosynthesis protein (Pbp), glycogen synthase (Gs), glycosyl transferase (Gt), bacterioferritin (*bfr*) and iron transport proteins (*feo*) in treated biofilms. Differences were statically obtained when compared to the control (*P < 0.05, **P < 0.01, ****P < 0.0001), (n = 3).

### 3.8. Phage-host interactions

To analyze the action of phage vB_EcoM-UFV13 on consortium P48SEP, the optical density of the consortium was monitored. No changes in optical density were observed in treatments with low and medium phage concentrations during the analyzed period compared to the control. However, treatment with $10^{12}$ PFU/mL reduced bacterial growth compared to the other treatments and control. Conversely, no difference was observed in the *O. marinus* and *O. teriensis* growth in the presence of phage at the three different concentrations evaluated (Fig. 7A).

Different from the observed in the consortium, the phage did not have a productive infection when each bacterial isolate was cultured alone. The ability of phage to replicate in the consortium indicates the necessity of a co-culture to perform a productive infection (Fig. 7B).

### 3.9. Pilot-scale assay

This experiment showed that the effect observed in the P48SEP consortium is more common than previously thought. Adding phages to the complex culture causes a reduction of $H_2S$, optical density, and metabolic activity (Fig. 8). The $H_2S$ production increases 1 day after the nutrient solution addition for tanks 2 and 3, while tank 1 increases on the same day. One day after phage inoculum (day 10), tank 2 reduced the $H_2S$ rate (Fig. 8A). All tanks increased until day 12, except tank 2, which received the bacteriophage UFV13. All tanks start to increase the $OD_{600}$ one day after the nutrient solution, with tanks 1 and 3 to continues to increase until day 13.

On the other hand, the UFV13 treatment (tank 2) had a consistent reduction on the same day of the phage inoculum (day 10), not reaching the concentration values of the other tanks (Fig. 8B). Unlike $H_2S$ concentration, the UFV13 phage inoculum caused an increase in the mercaptans concentration (Fig. 8C), which was not observed in tank 1 and delayed in 3. The UFV13 phage also caused a reduction in the metabolic status of the culture, evidenced by ATP reduction, not observed in the other 2 tanks (Fig. 8D).

## 4. Discussion

In this work, we describe for the first time the influence of a non-specific *Escherichia coli*-infecting phage on a culture consortium formed by two bacteria able to reduce sulfurated molecules, an ordinary sulfate-reducing bacterium, *O. marinus*, and the *O. teriensis*. This capability was confirmed in a pilot-scale experiment using a complex culture obtained from an oil exploring environment.

From phylogenetic analysis, it is possible to verify that the bacterial isolates groups with the species *Oceanotoga teriensis* OCT74$^T$ and *O. marinus*. This demonstrates that the bacterial consortium P48SEP consists of the species *O. marinus*, a representative of the group of sulfate-reducing bacteria (SRB), and *O. teriensis*, a species able to reduce sulphurated compounds. The *O. teriensis* OCT74$^T$ was isolated from a production water sample collected in offshore oil exploration and initially characterized. It is an anaerobic, Gram-negative, rod-shaped presenting a sheath-like outer structure ('toga'), chemoorganotrophic, multiple flagellated bacterium, with the ability to grow using different carbon sources and to reduce thiosulfate and elemental sulfur to hydrogen sulfide [45]. *O. marinus* was first isolated from marine sediments in Tunisia. Gram-negative, non-sporulated, motile, vibrio-shaped or sigmoid, strictly

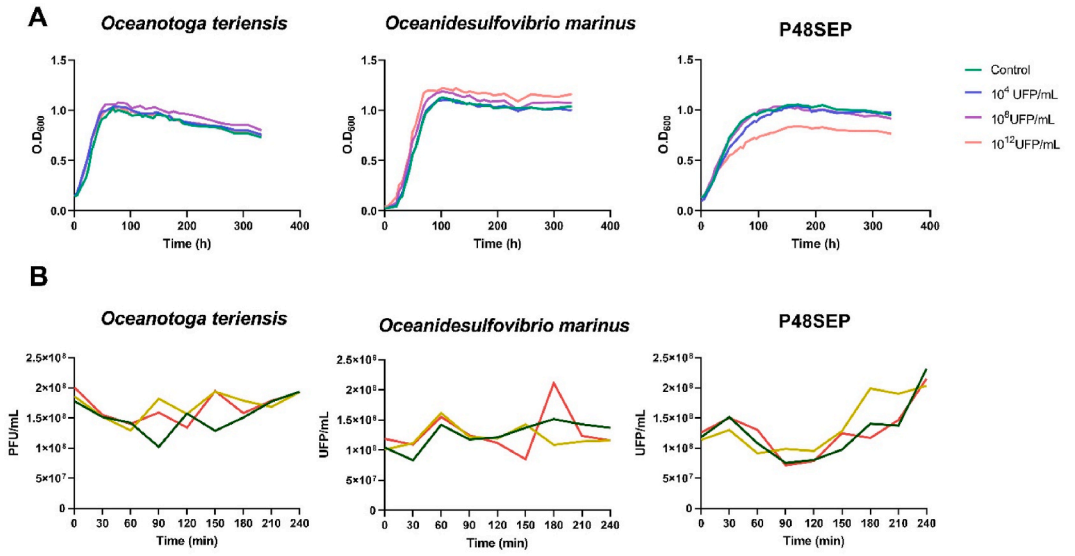


**Fig. 7. Phage-host interaction.** A) Bacterial growth curve in the presence of different phage concentrations. The bacterial isolates (*Oceanidesulfovibrio marinus* and *Oceanotoga teriensis*) and consortium (P48sep) growth curves are presented. B) Replication curve of phage vB_EcoM-UFV13 in the isolates and consortium. The supernatant was filtered and titrated in *E. coli* 30. Graphs represent 3 experiments (1, 2, and 3) performed in triplicate.

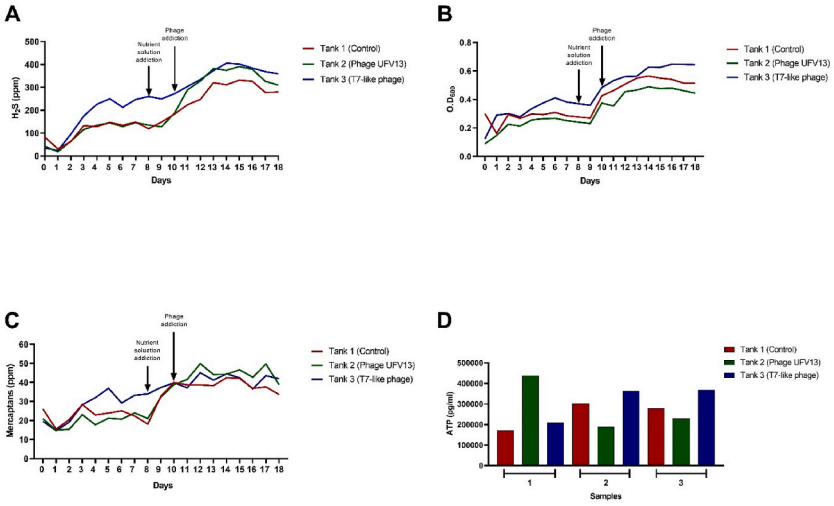


**Fig. 8. Pilot assay.** In the pilot, the assay evaluated 4 parameters of bacterial metabolism. A) $H_2S$ concentration, B) Optical density (OD), C) Mercaptans, and D) adenosine triphosphate (ATP). The ATP was sampled at the beginning of the experiment (1), one day after phage inoculum (2), and at the end of the experiment (3). The ATP assay presented significant differences in almost all pair comparisons, except for Tank 3 in samples 2 and 3.

anaerobic, mesophilic, and moderately halophilic. It uses sulfate, sulfite, thiosulfate, and elemental sulfur as electron acceptors but not nitrate or nitrite. Overall, $H_2$ (with acetate as a carbon source), formate, fumarate, lactate, malate, pyruvate, succinate, and fructose can be used as electron donors in the presence of sulfate as a terminal electron acceptor. *O. marinus* is capable of incompletely oxidizing lactate to acetate, while fumarate and pyruvate are fermented [46].

The most conventional methods to assess phage activity are the double-layer assay and spot assay, which permit visualization of the lysis plaques, but these techniques are laborious and time-consuming, especially for fastidious bacteria. An alternative to indirectly assess the lytic activity is monitoring the optical density. The cell concentration estimated by the optical density has the advantage of being faster and does not lose the sample [47]. Bacterial growth monitoring provides essential information about cellular physiology, such as nutritional and energetic characteristics, and enables a better understanding of survival and proliferation conditions under different treatments [48]. The reduction in the optical density of the bacterial culture in the presence of a lytic phage is indicative of cell lysis or metabolic activity reduction. However, it is necessary to highlight the use of the growth curve to estimate that bacterial activity has some flaws related to the stationary phase [49]. This work observed the reduction in the bacterial growth curve only at higher phage concentrations and only in the consortium, no effect was observed on the *O. teriensis* and *O. marinus* curves in the presence of phages at different concentrations. This behavior the need for a second bacterial species, that is, the bacterial consortium, so that the phage has a productive infection and can cause bacterial lysis. This effect can be explained by the characteristic of phages T4 infection, which interferes in the host's cellular machinery [50], as Fazzino, Anisman [51] showed to lytic phages, which can act dramatically on bacterial communities that are cross-fed, altering the metabolism of non-host species through multiple mechanisms. The attack on host species by lytic phage promotes changes in the metabolite levels available in the medium, reducing community growth. The exact multiplicity of infection (MOI) was impossible to determine since bacterial cell count presents inconsistency due to the colony (CFU) being shared by the two bacteria of the consortium; from flow cytometry analysis, we could determine that bacterial consortium presented a specific ratio formed by approximately 76 % *Oceanotoga teriensis* e 24 % *Oceanidesulfovibrio marinus* (data not shown). Furthermore, MOI is not recommended to be used in phage therapy experiments due to the difficulty of being established in some experiments [52].

The RT-PCR analysis clarifies the phage genes' role in bacterial growth reduction and showed that several phage genes were transcribed, with the exception of the sigma factor (Supplementary Fig. 2), which is central in late gene transcription (most structural proteins, e.g., tail, fiber, and head). Although *cap* and *tail* gene expression could be detected, the lack of sigma factor can be related to the inability of phage to cause bacterial lysis without the presence of a second species. Several phage genes are described to affect bacterial metabolic pathways, such as altering membrane lipid biosynthesis and degrading host DNA [50]. These characteristics show that *O. marinus* UFV_LIMV02 is susceptible to infection by the UFV13 phage, but becomes susceptible and permissive to the phage in the presence of the bacteria *O. teriensis*.

The treatment with high phage concentration was adequate to prevent the appearance of cracks in the metal surface and reduce the biofilm on the surface of the coupon. Several studies demonstrated that the SRB activity accelerates metal cracking, and some different roles are described. In the first role, SRB removes $H^0$ from the steel surface, which lowers the concentration and suppresses the $H^0$ permeation, which reduces crack propagation. However, although it is the core of the widely accepted cathodic depolarization theory of MIC induced by SRB, it is not accepted by all researchers. The second role is described as producing sulfur ions ($S^{2-}$) in the external environments, which recombine with $H^0$ and avoid $H_2$ forming, allowing the hydrogen atoms to diffuse to the plastic zone of the cracks, causing the steel's embrittlement. More recent literature describes other processes, chemical-MIC (CMIC) and electrical-MIC

(EMIC), which drive iron corrosion in sulfate-containing anoxic environments. EMIC occurs by direct electron uptake and was observed in only a few highly corrosive SRB isolates. On the other hand, SRB can influence corrosion by excreting the chemical $H_2S$ (CMIC) if sulfate and suitable electron donors are present [42,53–55].

Besides the crack reduction observed at treatments with phage at $10^4$ and $10^8$ PFU/mL, the phage UFV13 application decreased the biofilm formation in medium and high phage concentrations. Similar results were reported for controlling biofilms formed by *Trueperella pyogenes*, a non-host species, using phage vB_EcoM-UFV13. The eight proteins with hydrolase domains (VAPHs) on the phage genome were related to biofilm prevention by acting in the biofilm adhesion [23]. They can degrade the cell wall components of bacteria present in the P48SEP consortium and the EPS of the biofilm, as previously described [56,57]. The main components present in the biofilm matrix (polysaccharides, proteins, and extracellular DNA) provide several benefits to organisms present in this environment, including protection against antimicrobial agents and facilitating the surface adhesion process [44,58,59], and were also reduced. Although, in this case, bacterial cells are not killed by hydrolases, the destabilization of the biofilm structure due to the degradation of the main components that assist in the cell adhesion process leads to a decrease in the bacterial count present in the biofilm [60]. Thus, the enzymatic degradation of the main components of the extracellular matrix can be an essential strategy in controlling and preventing biocorrosion in metallic structures used in offshore oil exploration.

While bacteria are constantly evolving, creating mechanisms of resistance to bacteriophages, one of which is the blocking of cellular receptors through polysaccharide capsules that protect the entire bacterial surface [61]; in response, some phages have enzymes on their tails, such as hydrolases, capable of degrading this protection [62–64]. Consequently, when no sufficient enzyme types are present, an increase in the expression of genes related to the synthesis of capsules could explain the increase observed in the sugar present in the biofilm treated with a low phage concentration (Fig. 5A).

As with the matrix components, some bacterial proteins were affected by phage treatment. Flagellin is present in relevant quantities only in the presence of phage, which may be a bacterial response to phage action on the biofilm or adhesion molecules. This protein is a component of the flagella and is associated with the initial microorganisms' adhesion process to the surfaces [65]. There was no statistically significant change (albeit a reduction can be observed at higher phage concentrations) in the relative abundance of the *O. teriensis* S-layer in the presence of bacteriophage (Fig. 7). The S-layer has a crucial role in the emergence of resistant bacteria to phage attack by blocking the phage from reaching bacterial surface receptors, making them inaccessible to the phage receptor binding proteins [66]. The concentrations of outer membrane proteins (Omp), extracellular ligand-binding receptor, and peptide/nickel transport system substrate-binding and ABC transport proteins did not differ in relative abundance. Such proteins are possible cellular receptors and carrier viral genetic material after phage adsorption [66,67]. The proteins sulfate adenyltransferase and sulfite reductase had their relative abundance levels increased in the presence of phage vB_EcoM-UFV13 (Fig. 7). These two proteins are part of the sulfate reduction pathway in *Oceanidesulfovibrio* ssp., which is used to obtain energy from the organic compounds or hydrogen oxidation (electron donors) coupled to sulfate reduction, with hydrogen sulfide as a final product [68,69]. Briefly, sulfate is activated with the expense of two ATP molecules through the activity of sulfate adenylyltransferase (*sat*), producing adenosine-5′-phosphosulfate (APS). APS is reduced by APS reductase (*apr*), generating sulfite and AMP. Finally, a reduction of six electrons from sulfite to sulfide occurs using hydrogen as the electron source through dissimilatory sulfite reductase (*dsr*) coupled with oxidative phosphorylation [70,71]. Some proteins or protein families found augmented in this work are related to sulfide accumulation response, such as iron compound ABC transporter, nickel ABC transport system (NikO), and ferrous iron transport protein B [72]. Despite this increase in some proteins, phage-treated samples showed different protein-produced patterns and gene expression compared to control. Similar results were found when biocides were used as stressors [73]. Future studies are needed to evaluate whether the presence of phage caused an increase in the energy demand of cells, which consequently promoted an increase in the expression of enzymes involved in the sulfate reduction pathway.

Finally, a decrease in the relative abundance of 60 kDa chaperonin in the biofilm was observed in the presence of phage vB_EcoM-UFV13 (Fig. 6). This protein mainly prevents inappropriate association between subunits and protein domains during the folding process and facilitates their correct folding [74]. However, studies using *E. coli* that have mutations in the 60 kDa chaperonin-encoding gene have been unable to propagate T4 and T5 phages, showing that this protein is essential for bacteriophage assembly [75,76]. The decrease in chaperonin expression is a cell strategy to prevent the correct folding of its proteins and, consequently, the phage proteins to avoid the release of new phage progeny. Some cells activate the programmed death by disrupting essential cellular processes, such as translation, transcription, and replication, or by inducing membrane leakage to prevent the release of new phages and the consequent spread of phages to the surrounding bacterial population; this process is known as an abortive infection [61].

At lower concentrations, vB_EcoM-UFV13 was able to alter the gene expression levels of all analyzed genes. The low viral load probably triggered an adaptive response to the phage's antimicrobial action, altering the gene expression pattern related to exopolysaccharide biosynthesis, as observed elsewhere [77,78]. Bacteria use this mechanism to block the process of virus adsorption by promoting receptor concealment through a physical barrier [23,67]. The results agree with what had already been observed in sugar quantification (Fig. 5A), in which there was an increase in the carbohydrate amount present in the biofilm when using the phage at $10^4$ PFU/mL.

The increase in the abundance of proteins related to the transport and storage of iron has already been reported in other studies with biofilm [79–81], showing that high levels of iron signalize *Pseudomonas aeruginosa* the formation of microcolonies and eventually ripen biofilms. In contrast, low iron levels discourage biofilm growth [79,82].

The relationship between bacteria and phages constantly evolves, meaning bacteria evolve by creating and improving anti-phage mechanisms, while phages adapt to overcome these apparatuses [61]. The presence of phages in the biofilm triggered the bacterial defense system to prevent the stages of the phage life cycle, such as blocking cell receptors to prevent adsorption and injection of the genetic material of the phages by increasing the production of carbohydrates; otherwise, it was through the disturbance of essential

cellular processes, such as translation and transcription.

The pilot-scale experiment showed the effect of this phage on a complex culture. After phage addition, the culture metabolism was strongly reduced, and the condition was maintained until the experiment ended. The phage affects some bacterial populations, which can be related to reduced $H_2S$ production with a concomitant increase in the mercaptan's production. Different bacterial groups produce these compounds. This behavior has been previously reported for lytic phages [51]. However, this is the first time it has been described as a lytic phage acting in a complex culture without the presence of the original host. The metabolic interdependence of different bacterial groups in the sulfur cycle is known [83], and the role of different bacterial groups on mercaptans (methyl mercaptan) and $H_2S$ production in a different environment (oral microbiota) was also described [84]. The T4-like phages can take over the host metabolism [50] and belong to a ubiquitous virus superfamily, in which the specificity is determined by a complex modular adhesin, a protein designed to exploit a set of modular recognition sequences sophisticatedly. Besides, previous work demonstrates the dominance of prophages classified to the extinct family Myoviridae in the genomes of the *Oceanidesulfovibrio* genus [85].

Although further investigation is needed to understand all of the metabolic changes involved in bacterial growth reduction, this study showed that medium ($10^8$ PFU/mL) and high ($10^{12}$ PFU/mL) administration of vB_EcoM-UFV13 was able to prevent the formation and development by consortium P48SEP. In addition, such viral concentrations promoted a decrease in the main molecules responsible for bacteria adhesion and the biofilm stabilization processes. The phage also reduced the number of living cells present in the biofilm. This work shows for the first time the ability of an *E. coli*-specific bacteriophage to prevent biofilm formation from SRB. It reduces the metabolic state of a complex community formed by SRB, a promising alternative for biocorrosion control in oil pipelines and storage tanks.

## Funding

This research was funded by PETROBRAS, FAPEMIG, and CNPq.

## Data availability statement

The authors declare that all data have been included in the article/supplementary material/referenced in the article.

## CRediT authorship contribution statement

**Adriele Jéssica do Carmo Santos:** Methodology, Investigation, Data curation, Conceptualization. **Roberto Sousa Dias:** Writing – review & editing, Writing – original draft, Formal analysis, Conceptualization. **Jéssica Duarte Silva:** Methodology, Investigation. **Maíra de Paula Sousa:** Resources, Data curation, Conceptualization. **Wellington Ronildo Clarindo:** Methodology, Investigation. **Cynthia Canêdo da Silva:** Writing – original draft, Resources, Project administration. **Sérgio Oliveira de Paula:** Writing – review & editing, Supervision, Resources, Project administration, Data curation, Conceptualization.

## Declaration of competing interest

The authors declare that they have no known competing financial interests or personal relationships that could have appeared to influence the work reported in this paper.

## Acknowledgments

The authors are grateful to PETROBRAS, FAPEMIG, CNPq, and CAPES for the financial support and the granting of scholarships.

## Appendix A. Supplementary data

Supplementary data to this article can be found online at https://doi.org/10.1016/j.heliyon.2024.e37934.

## References

[1] C. Zou, et al., Energy revolution: from a fossil energy era to a new energy era, Nat. Gas. Ind. B 3 (1) (2016) 1–11.
[2] F.M. AlAbbas, et al., Influence of sulfate reducing bacterial biofilm on corrosion behavior of low-alloy, high-strength steel (API-5L X80), Int. Biodeterior. Biodegrad. 78 (2013) 34–42.
[3] N. Kip, J.A. van Veen, The dual role of microbes in corrosion, ISME J. 9 (3) (2015) 542–551.
[4] J. Reza, Microbiologically Influenced Corrosion an Engineering Insight, Springer-Verlag, London Limited, 2008.
[5] B.J. Little, J.S. Lee, Microbiologically Influenced Corrosion, vol. 3, John Wiley & Sons, 2007.
[6] J.L. Balcázar, J. Subirats, C.M. Borrego, The role of biofilms as environmental reservoirs of antibiotic resistance, Front. Microbiol. 6 (2015), 1216-1216.
[7] S.J. Yuan, S.O. Pehkonen, AFM study of microbial colonization and its deleterious effect on 304 stainless steel by Pseudomonas NCIMB 2021 and Desulfovibrio desulfuricans in simulated seawater, Corrosion Sci. 51 (6) (2009) 1372–1385.
[8] H. Dang, C.R. Lovell, Microbial surface colonization and biofilm development in marine environments, Microbiol. Mol. Biol. Rev. : MMBR (Microbiol. Mol. Biol. Rev.) 80 (1) (2015) 91–138.

[9] G. Muyzer, A.J. Stams, The ecology and biotechnology of sulphate-reducing bacteria, Nat. Rev. Microbiol. 6 (6) (2008) 441–454.
[10] D.J. Blackwood, An electrochemist perspective of microbiologically influenced corrosion, Corrosion and Materials Degradation 1 (1) (2020) 59–76.
[11] M. Nemati, G.E. Jenneman, G. Voordouw, Mechanistic study of microbial control of hydrogen sulfide production in oil reservoirs, Biotechnol. Bioeng. 74 (5) (2001) 424–434.
[12] D. Xu, Y. Li, T. Gu, Mechanistic modeling of biocorrosion caused by biofilms of sulfate reducing bacteria and acid producing bacteria, Bioelectrochemistry 110 (2016) 52–58.
[13] S.M. Bhola, et al., Neem extract as an inhibitor for biocorrosion influenced by sulfate reducing bacteria: a preliminary investigation, Eng. Fail. Anal. 36 (2014) 92–103.
[14] B. Little, J. Lee, R. Ray, A review of 'green' strategies to prevent or mitigate microbiologically influenced corrosion, Biofouling 23 (1–2) (2007) 87–97.
[15] C. Ferriol-González, P. Domingo-Calap, Phages for biofilm removal, Antibiotics (Basel) 9 (5) (2020).
[16] I.W. Sutherland, et al., The interaction of phage and biofilms, FEMS Microbiol. Lett. 232 (1) (2004) 1–6.
[17] R. Pei, G.R. Lamas-Samanamud, Inhibition of biofilm formation by T7 bacteriophages producing quorum-quenching enzymes, Appl. Environ. Microbiol. 80 (17) (2014) 5340–5348.
[18] D.P. Pires, et al., Bacteriophage-encoded depolymerases: their diversity and biotechnological applications, Appl. Microbiol. Biotechnol. 100 (5) (2016) 2141–2151.
[19] J. Yan, J. Mao, J. Xie, Bacteriophage polysaccharide depolymerases and biomedical applications, BioDrugs 28 (3) (2014) 265–274.
[20] E.J. Summer, et al., Phage of sulfate reducing bacteria isolated from high saline environment. In: NACECOrrosion. Paper No, 11222, NACE International, Houston, 2011, pp. 1–12.
[21] I. Kushkevych, et al., Microscopic methods for identification of sulfate-reducing bacteria from various habitats, Int. J. Mol. Sci. 22 (8) (2021) 4007.
[22] D.W. Waite, et al., Proposal to reclassify the proteobacterial classes Deltaproteobacteria and Oligoflexia, and the phylum Thermodesulfobacteria into four phyla reflecting major functional capabilities, Int. J. Syst. Evol. Microbiol. 70 (11) (2020) 5972–6016.
[23] V. da Silva Duarte, et al., A T4virus prevents biofilm formation by Trueperella pyogenes, Vet. Microbiol. 218 (2018) 45–51.
[24] V.S. Duarte, et al., Complete genome sequence of vB_EcoM-UFV13, a new bacteriophage able to disrupt Trueperella pyogenes biofilm, Genome Announc. 4 (6) (2016).
[25] C. Desplats, H.M. Krisch, The diversity and evolution of the T4-type bacteriophages, Res. Microbiol. 154 (4) (2003) 259–267.
[26] J.R. Postgate, The Sulphate-Reducing Bacteria, CUP Archive, 1979.
[27] A. Pospiech, B. Neumann, A versatile quick-prep of genomic DNA from gram-positive bacteria, Trends Genet. 11 (6) (1995) 217–218.
[28] D. Lane, 16S/23S rRNA sequencing, in: E. Stackebrandt, M. Goodfellow (Eds.), Nucleic Acid Techniques in Bacterial Systematics, John Wiley and Sons, Chichester, UK, 1991, pp. 115–175.
[29] J.D. Thompson, et al., The CLUSTAL_X windows interface: flexible strategies for multiple sequence alignment aided by quality analysis tools, Nucleic Acids Res. 25 (24) (1997) 4876–4882.
[30] K. Tamura, et al., MEGA4: molecular evolutionary genetics analysis (MEGA) software version 4.0, Mol. Biol. Evol. 24 (8) (2007) 1596–1599.
[31] J. Sambrook, E.F. Fritsch, T. Maniatis, Molecular Cloning: a Laboratory Manual, Cold spring harbor laboratory press, 1989.
[32] V.S. Liduino, M.T.S. Lutterbach, E.F.C. Sérvulo, Biofilm activity on corrosion of API 5L X65 steel weld bead, Colloids Surf. B Biointerfaces 172 (2018) 43–50.
[33] R. Wang, et al., Inhibition of Escherichia coli and Proteus mirabilis adhesion and biofilm formation on medical grade silicone surface, Biotechnol. Bioeng. 109 (2) (2012) 336–345.
[34] S. Jachlewski, et al., Isolation of extracellular polymeric substances from biofilms of the thermoacidophilic archaeon sulfolobus acidocaldarius, Front. Bioeng. Biotechnol. 3 (2015), 123-123.
[35] M. Dubois, et al., Colorimetric method for determination of sugars and related substances, Anal. Chem. 28 (3) (1956) 350–356.
[36] Y. Ishihama, et al., Exponentially modified protein abundance index (emPAI) for estimation of absolute protein amount in proteomics by the number of sequenced peptides per protein, Mol. Cell. Proteomics 4 (9) (2005) 1265–1272.
[37] M. Zago, et al., Survey on the phage resistance mechanisms displayed by a dairy Lactobacillus helveticus strain, Food Microbiol. 66 (2017) 110–116.
[38] P.A. Mosier-Boss, et al., Use of fluorescently labeled phage in the detection and identification of bacterial species, Appl. Spectrosc. 57 (9) (2003) 1138–1144.
[39] M.S. Vieira, et al., A highly specific Serratia-infecting T7-like phage inhibits biofilm formation in two different genera of the Enterobacteriaceae family, Res. Microbiol. 172 (6) (2021) 103869.
[40] V. Blanes-Vidal, et al., Emissions of NH3, CO2 and H2S during swine wastewater management: characterization of transient emissions after air-liquid interface disturbances, Atmos. Environ. 54 (2012) 408–418.
[41] A. Selvy, Impacts of Ozone Dose and Empty Bed Contact Time on Total Organic Carbon Removal through Ozone-Biological Activated Carbon Treatment, 2015.
[42] C. Xu, et al., Pitting corrosion behavior of 316L stainless steel in the media of sulphate-reducing and iron-oxidizing bacteria, Mater. Char. 59 (3) (2008) 245–255.
[43] K. Naicker, S.I. Durbach, Epifluorescent microscopy to evaluate bacteriophage capsid integrity, Biotechniques 43 (4) (2007), 473-4, 476.
[44] D.H. Limoli, C.J. Jones, D.J. Wozniak, Bacterial extracellular polysaccharides in biofilm formation and function, Microbiol. Spectr. 3 (3) (2015), https://doi.org/10.1128/microbiolspec.MB-0011-2014.
[45] H.S. Jayasinghearachchi, B. Lal, Oceanotoga teriensis gen. nov., sp. nov., a thermophilic bacterium isolated from offshore oil-producing wells, Int. J. Syst. Evol. Microbiol. 61 (Pt 3) (2011) 554–560.
[46] O. Ben Dhia Thabet, et al., Desulfovibrio marinus sp. nov., a moderately halophilic sulfate-reducing bacterium isolated from marine sediments in Tunisia, Int. J. Syst. Evol. Microbiol. 57 (Pt 9) (2007) 2167–2170.
[47] M.R.G. Maia, et al., Simple and versatile turbidimetric monitoring of bacterial growth in liquid cultures using a customized 3D printed culture tube holder and a miniaturized spectrophotometer: application to facultative and strictly anaerobic bacteria, Front. Microbiol. 7 (2016), 1381-1381.
[48] M.C. Flickinger, Encyclopedia of Industrial Biotechnology: Bioprocess, Bioseparation, and Cell Technology, 7 Volume Set, john wiley & sons, 2010.
[49] O. Braissant, et al., A review of methods to determine viability, vitality, and metabolic rates in microbiology, Front. Microbiol. 11 (2020) 547458.
[50] E. Kutter, et al., From host to phage metabolism: hot tales of phage T4's takeover of E. coli, Viruses 10 (7) (2018).
[51] L. Fazzino, et al., Lytic bacteriophage have diverse indirect effects in a synthetic cross-feeding community, ISME J. 14 (1) (2020) 123–134.
[52] S.T. Abedon, Phage therapy dosing: the problem(s) with multiplicity of infection (MOI), Bacteriophage 6 (3) (2016) e1220348.
[53] T. Wu, et al., Sulfate-reducing bacteria-assisted cracking, Corrosion Rev. 37 (3) (2019) 231.
[54] D. Enning, J. Garrelfs, Corrosion of iron by sulfate-reducing bacteria: new views of an old problem, Appl. Environ. Microbiol. 80 (4) (2014) 1226–1236.
[55] R.C. Souza, et al., Effect of microstructure on hydrogen diffusion in weld and API X52 pipeline steel base metals under cathodic protection, International Journal of Corrosion 2017 (2017) 4927210.
[56] K.A. Hughes, I.W. Sutherland, M.V. Jones, Biofilm susceptibility to bacteriophage attack: the role of phage-borne polysaccharide depolymerase, Microbiology (Read.) 144 (Pt 11) (1998) 3039–3047.
[57] K.A. Hughes, et al., Bacteriophage and associated polysaccharide depolymerases–novel tools for study of bacterial biofilms, J. Appl. Microbiol. 85 (3) (1998) 583–590.
[58] J.N.C. Fong, F.H. Yildiz, Biofilm matrix proteins, Microbiol. Spectr. 3 (2) (2015), https://doi.org/10.1128/microbiolspec.MB-0004-2014.
[59] C.B. Whitchurch, et al., Extracellular DNA required for bacterial biofilm formation, Science 295 (5559) (2002) 1487.
[60] T.K. Lu, J.J. Collins, Dispersing biofilms with engineered enzymatic bacteriophage, Proc. Natl. Acad. Sci. U.S.A. 104 (27) (2007) 11197–11202.
[61] J.T. Rostøl, L. Marraffini, (Ph)ighting phages: how bacteria resist their parasites, Cell Host Microbe 25 (2) (2019) 184–194.
[62] H. Oliveira, C. São-José, J. Azeredo, Phage-derived peptidoglycan degrading enzymes: challenges and future prospects for in vivo therapy, Viruses 10 (6) (2018) 292.
[63] L.M.T. Dicks, W. Vermeulen, Bacteriophage-host interactions and the therapeutic potential of bacteriophages, Viruses 16 (3) (2024).

[64] B. Maciejewska, T. Olszak, Z. Drulis-Kawa, Applications of bacteriophages versus phage enzymes to combat and cure bacterial infections: an ambitious and also a realistic application? Appl. Microbiol. Biotechnol. 102 (6) (2018) 2563–2581.
[65] M. Zhou, et al., Flagellin and F4 fimbriae have opposite effects on biofilm formation and quorum sensing in F4ac+ enterotoxigenic Escherichia coli, Vet. Microbiol. 168 (1) (2014) 148–153.
[66] J. Bertozzi Silva, Z. Storms, D. Sauvageau, Host receptors for bacteriophage adsorption, FEMS (Fed. Eur. Microbiol. Soc.) Microbiol. Lett. 363 (4) (2016).
[67] F. Golais, J. Holly, J. Vitkovska, Coevolution of bacteria and their viruses, Folia Microbiol (Praha) 58 (3) (2013) 177–186.
[68] U. Kappler, C. Dahl, Enzymology and molecular biology of prokaryotic sulfite oxidation1, FEMS (Fed. Eur. Microbiol. Soc.) Microbiol. Lett. 203 (1) (2001) 1–9.
[69] P.M. Pereira, et al., Energy metabolism in Desulfovibrio vulgaris Hildenborough: insights from transcriptome analysis, Antonie Leeuwenhoek 93 (4) (2008) 347–362.
[70] K.L. Keller, et al., New model for electron flow for sulfate reduction in Desulfovibrio alaskensis G20, Appl. Environ. Microbiol. 80 (3) (2014) 855–868.
[71] M.E. Clark, et al., Transcriptomic and proteomic analyses of Desulfovibrio vulgaris biofilms: carbon and energy flow contribute to the distinct biofilm growth state, BMC Genom. 13 (2012) 138.
[72] S.M. Caffrey, G. Voordouw, Effect of sulfide on growth physiology and gene expression of Desulfovibrio vulgaris Hildenborough, Antonie Leeuwenhoek 97 (1) (2010) 11–20.
[73] M.H. Lee, et al., Effects of biocides on gene expression in the sulfate-reducing bacterium Desulfovibrio vulgaris Hildenborough, Appl. Microbiol. Biotechnol. 87 (3) (2010) 1109–1118.
[74] A. Brinker, F.U. Hartl, Chaperonins, in: S. Brenner, J.H. Miller (Eds.), Encyclopedia of Genetics, Academic Press, New York, 2001, pp. 324–325.
[75] C.P. Georgopoulos, B. Hohn, Identification of a host protein necessary for bacteriophage morphogenesis (the groE gene product), Proc. Natl. Acad. Sci. U.S.A. 75 (1) (1978) 131–135.
[76] R.W. Hendrix, Purification and properties of groE, a host protein involved in bacteriophage assembly, J. Mol. Biol. 129 (3) (1979) 375–392.
[77] E.K. Chu, et al., Self-induced mechanical stress can trigger biofilm formation in uropathogenic Escherichia coli, Nat. Commun. 9 (1) (2018) 4087.
[78] A.W. Qurashi, A.N. Sabri, Bacterial exopolysaccharide and biofilm formation stimulate chickpea growth and soil aggregation under salt stress, Braz. J. Microbiol. : [publication of the Brazilian Society for Microbiology] 43 (3) (2012) 1183–1191.
[79] A. Soldano, et al., Inhibiting iron mobilization from bacterioferritin in Pseudomonas aeruginosa impairs biofilm formation irrespective of environmental iron availability, ACS Infect. Dis. 6 (3) (2020) 447–458.
[80] P.K. Singh, et al., A component of innate immunity prevents bacterial biofilm development, Nature 417 (6888) (2002) 552–555.
[81] M.A. Pysz, et al., Transcriptional analysis of biofilm formation processes in the anaerobic, hyperthermophilic bacterium Thermotoga maritima, Appl. Environ. Microbiol. 70 (10) (2004) 6098–6112.
[82] T. Hindre, et al., Transcriptional profiling of Legionella pneumophila biofilm cells and the influence of iron on biofilm formation, Microbiology 154 (Pt 1) (2008) 30–41.
[83] J.C.d. Santos, et al., Diversity of sulfate-reducing prokaryotes in petroleum production water and oil samples, Int. Biodeterior. Biodegrad. 151 (2020) 104966.
[84] T. Takeshita, et al., Discrimination of the oral microbiota associated with high hydrogen sulfide and methyl mercaptan production, Sci. Rep. 2 (2012) 215.
[85] J.S. Crispim, et al., Screening and characterization of prophages in Desulfovibrio genomes, Sci. Rep. 8 (1) (2018) 9273.